Applied Surface Science 332 (2015) 694–698

Contents lists available at ScienceDirect

Applied Surface Science

journal homepage: www.elsevier.com/locate/apsusc

Resistivity and Hall voltage in gold thin films deposited on mica at room temperature

Sebastián Bahamondes [a], Sebastián Donoso [a], Antonio Ibañez-Landeta [a], Marcos Flores [a], Ricardo Henriquez [b,∗]

[a] Departamento de Física, Facultad de Ciencias Físicas y Matemáticas, Universidad de Chile, Av. Blanco Encalada 2008, Santiago, Chile
[b] Departamento de Física, Universidad Técnica Federico Santa María, Av. España 1680, Valparaiso 2390123, Chile

ARTICLE INFO

Article history:
Received 9 September 2014
Received in revised form
12 December 2014
Accepted 21 January 2015
Available online 29 January 2015

Keywords:
Resistivity
Hall voltage
Thin film
Gold

ABSTRACT

We report the thickness dependence of the resistivity measured at 4 K of gold films grown onto mica at room temperature (RT), for thickness ranging from 8 to 100 nm. This dependence was compared to the one obtained for a sample during its growth process at RT. Both behaviors are well represented by the Mayadas–Shatzkes theory. Using this model, we found comparable contributions of electron surface and electron grain boundary scattering to the resistivity at 4 K. Hall effect measurements were performed using a variable transverse magnetic field up to 4.5 T. Hall tangent and Hall resistance exhibit a linear dependence on the magnetic field. For this magnetic field range, the Hall mobility is always larger than the drift mobility. This result is explained through the presence of the above-mentioned scattering mechanisms acting on the galvanomagnetic coefficients. In addition, we report the temperature dependence of the resistivity between 4 and 70 K.

© 2015 Elsevier B.V. All rights reserved.

1. Introduction

Metallic films deposited on insulating substrates are one of the most used systems in the study of optical, magnetic, mechanical and electrical properties of metals [1]. Control over sample thickness and microstructure, through modification of growth conditions, increases the usefulness of these systems. Among them, gold thin films on an insulating substrate are one of the most used due to easy fabrication and to the null oxidation at atmospheric conditions [2].

From the point of view of electrical transport, in gold thin films at room temperature, a series of scattering mechanisms participates increasing the resistivity: electron phonons scattering, electron grain boundary scattering and electron surface scattering. Some reports show experimentally the effect of each mechanism. Some examples, Kastle et al. [3] and Henriquez et al. [4] reported gold thin films where the dominant mechanism is electron surface scattering. They found that the temperature dependence of the resistivity exhibits an increase of its slope respect to that of the bulk. On the other hand, when the dominant mechanism is electron grain boundary scattering this increase is not observed, and also, the mean free path at 4 K correspond to mean grain diameter [5].

Deposition of thin gold films at room temperature results in samples characterized by a mean grain diameter comparable to the film thickness. Also, this dimension increases as thickness grows. Some examples of these morphological conditions: thin gold films on mica [2], on SiO_2 [6] and on glass [7]. Thereby, these samples present an opportunity to study the effect of both mechanisms, electron surface scattering and electron grain boundary scattering, acting on the resistivity and on the galvanomagnetic coefficients.

In this work, we studied the resistivity, magnetoresistance and Hall voltage and its relation to the microstructure, in a set of gold thin films where the electron grain boundary scattering and electron surface scattering affect the charge transport process.

2. Experimental

We deposited thin gold films onto freshly cleaved mica through thermal evaporation at room temperature. Starting from 99.9999% pure gold, we evaporated at 1.2 nm/min from a tungsten basket in a High Vacuum chamber (10^{-4} Pa). A quartz microbalance located close to the sample monitored the evaporation rate. Mica surface roughness is about 0.3 nm over areas of 1 μm × 1 μm. Sample thickness was measured by Tolansky Optical Interferometry performed over test samples on glass slides placed close to the mica substrate.

∗ Corresponding author.
E-mail addresses: ricardo.henriquez@usm.cl, rahc.78@gmail.com (R. Henriquez).

http://dx.doi.org/10.1016/j.apsusc.2015.01.166
0169-4332/© 2015 Elsevier B.V. All rights reserved.

Thicknesses are consistent with values measured by the quartz microbalance.

Morphology of the gold films was characterized through scanning tunneling microscopy (STM) at room temperature (RT) in air using Pt-Ir tips. Images were processed with linear plane fit in order to remove the tilt with WSxM [8] before the statistical analysis. Using ImageJ software we marked grain boundaries and measured the enclosing area. We measured over 500 grains per sample to ensure a representative value [9]. Then, the characteristic size of a grain is the diameter of a circle enclosing the mean area.

Regarding to electrical characterization, in all samples we used the 4-contact method. We performed three different measurements:

(a) Determination of the temperature dependence of the resistivity between 4 and 70 K. Samples were located in a copper block inserted in a superconducting Magnet built by Janis Research Co. The electrical measurement started when the standard deviation of the temperature was smaller than 0.1 K. Films were fed with alternate current of 210 Hz and smaller than 500 μA. Voltages signal were acquired using computer controlled 830's LIA built by Stanford Research.
(b) Determination of magnetoresistance and Hall Voltage at 4.2 K. Experimental set up is similar to (a), but samples were immersed in magnetic fields up to 4.5 T. To measure the Hall voltage, we used the five-contact method, seeking to null the transverse signal in the absence of a magnetic field. Details of the method can be found elsewhere [10]
(c) Determination of the resistance during the evaporation process at RT. We pre-evaporated gold contacts on mica, and measured the resistance during the film evaporation. The sample was fed with direct current, alternating the polarity each 4 s approximately. Voltages were acquired through Nanovoltmeters built by Keithley.

3. Theory

3.1. Resistivity

In 1970, Mayadas and Shatzkes (MS) published the first theory of resistivity including the effect of both electron-grain boundary and electron-surface scattering [11]. The theory describes the electron motion using a Boltzmann Transport Equation. Grain boundaries are represented by a series of Dirac δ function potentials and characterized by a reflectivity coefficient R. This coefficient represents the fraction of electron reflected specularly at the grain boundary. The distance separating the Dirac δ function potentials is distributed following a Gaussian, characterized by an average separation d and a standard deviation s. The effect of electron-surface scattering on the resistivity is introduced through a specularity coefficient P based on Fuchs-Sondheimer theory [12]. This coefficient is imposed on the electron distribution function as a boundary condition at the interfaces that limit the metallic film. $(1-P)$ represents the fraction of the charge carrier scattered by the surface, which induce an increase on the resistivity. We modified this boundary condition allowing two different specularity parameters P and Q, associated to the upper and lower interface, respectively, following the work published by Lucas [13]. Finally, the expression to calculate the resistivity increase ρ_F/ρ_0 (where ρ_F represents the film resistivity and ρ_0, the bulk resistivity), depend on seven parameters: d, s, R, P, Q, t and ℓ_0. The last two symbols represent the thickness and the bulk mean free path, respectively. The final expression used for calculating the resistivity was published elsewhere [4,5]

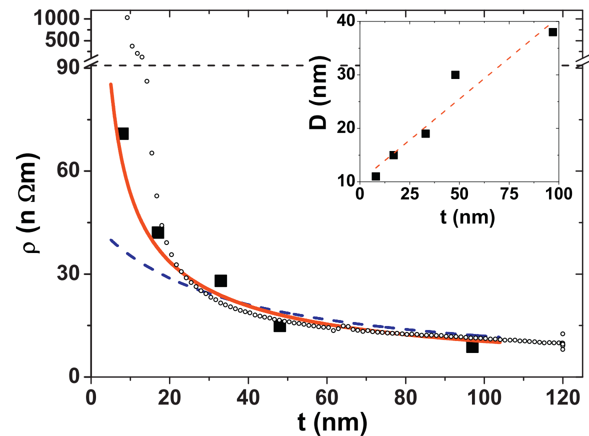

Fig. 1. Thickness dependence of the resistivity at 4 K. Squares represent the experimental data. Empty circles represent the resistivity determined by the in situ measurement of the resistance during the evaporation process at room temperature. An offset was subtracted to get the resistivity at 4 K in the same sample. Continuous and dashed lines represent the best fit obtained by Mayadas–Shatzkes–Lucas theory (MSL), for $(R, P, Q) = (0.18, 0.0, 0.0)$ and $(0.24, 0.0, 1.0)$, respectively. Inset: Thickness dependence of the mean grain diameter for the samples labeled with squares. Dashed line represents the linear dependence used in MSL.

3.2. Magnetoresistance and Hall voltage

In this work, we study the transverse magnetoresistance $\Delta\rho/\rho = [\rho(B) - \rho(B \equiv 0)]/\rho(B \equiv 0)]$, where $\rho(B)$ represents the resistivity when the sample is immersed in a transverse magnetic field B. To our knowledge, there is not a theory including electron-grain boundary scattering, electron-surface scattering and magnetic field describing the magnetoresistance in thin metallic films. Then, the classical interpretation of the effect of the magnetic field on the conduction electrons will be considered. The trajectories between scattering events are modified due to the curvature induced by the magnetic field. A measurement of this is the fraction of cyclotron orbit performed by the conduction electrons $\omega\tau$, where τ is the scattering time and $\omega = qB/m$ (q and m are the charge and mass of conduction electrons, respectively, and B, the magnetic field). If $(\omega\tau) \ll 1$, then the effect should be weak. In this case, magnetoresistance is proportional to $(\omega\tau)^2$, i.e., there is a quadratic dependence on the magnetic field.

Regarding the Hall voltage, the drift velocity v_D of the electrons in presence of the electric field $\mathbf{E}$, can be expressed as $\mathbf{E}$, where $v_D = \mu_D\mathbf{E}$, where μ_D represents the drift mobility. To add a magnetic field $\mathbf{B}$, the Lorentz force on the conduction electrons modify the drift velocity such that $v_D = \mu_D\mathbf{E} + \mu_D\mu_H\mathbf{E} \times \mathbf{B}$, where μ_H represents the Hall mobility. In the particular case where $\mathbf{E} = (E_X, E_Y, 0)$ and $\mathbf{B} = (0, 0, B)$, canceling the component v_{DY} of the drift velocity leads to the Hall tangent $tg(\theta) = E_{Hall}/E_{Longitual} = \mu_H B$ On the other hand, if we only want to compare the Hall voltage from different samples, the Hall resistance $R_H = V_H/I$ is often used, where I is the current feeding the sample.

4. Results

A resume of the morphological and electrical characterizations of gold thin films appears in Table 1.

Fig. 1 shows the thickness dependence of the resistivity at 4 K. Using Mayadas–Shatzkes–Lucas theory (MSL), we adjusted experimental data following procedure outlined below. First, we adjusted the thickness dependence of the mean grain diameter $d(t)$ from experimental data determined by STM. Inset of Fig. 1 shows the thickness dependence of the mean grain diameter and the linear regression: $d(t) = 0.31t + 10.14$ (d and t in nanometer).

Table 1
Morphological and electrical characterization of the samples. t: film thickness. D: mean grain diameter. ΔD: standard deviation of D. $\rho(4)$: film resistivity at 4 K. R: reflectivity parameter of grain boundary. $\mu_D(4)$: drift mobility at 4 K. $\mu_H(4)$: Hall mobility at 4 K. $\omega\tau(4.5)$ fraction of cyclotron orbit performed at 4 K and 4.5 T.

t (nm)	D (nm)	ΔD (nm)	$\rho(4)\times 10^{-9}(\Omega\mathrm{m})$	R	$\mu_D(4)\times 10^{-3}$ (m²/V s)	$\mu_H(4)\times 10^{-3}$ (T⁻¹)	$\omega\tau(4.5)$
8	11	3	70.9	0.21	1.5	–	–
17	15	8	42.1	0.22	2.5	3.4	0.015
33	19	7	28.0	0.22	3.8	6.8	0.031
47	30	13	14.9	0.14	7.1	8.6	0.039
97	39	17	8.81	0.16	12	13	0.059

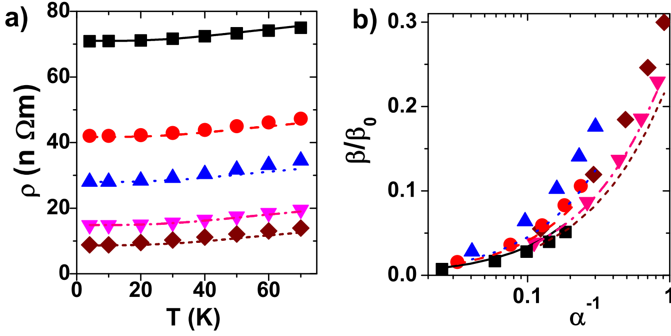

Fig. 2. (a) Temperature dependence of the resistivity. Solid symbols represent experimental data. Squares, circles, triangles, inverted triangles and diamonds, correspond to the samples 8, 17, 33, 47 and 97 nm thick, respectively. Lines represent the MSL prediction, adjusting the resistivity at 4 K, and adding the temperature dependent term predicted by Bloch-Gruneissen for gold bulk. (b) Ratio of the film tcr to the bulk tcr as a function of the inverse of the α parameter, at 30, 40, 50, 60 and 70 K. Solid symbols are the same as in a). Continuous, dashed, dotted, dash-dotted and short dashed lines represent the theoretical prediction from Ref. 15, for the samples 8, 17, 33, 47 and 97 nm thick, respectively.

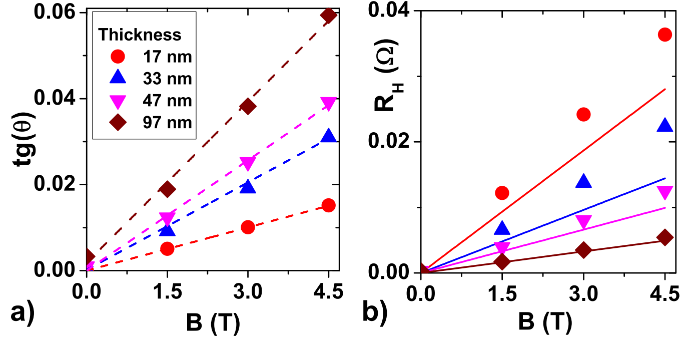

Fig. 3. Magnetic field dependence of the (a) Hall tangent and (b) Hall resistance for 17, 33, 47 and 97 nm thick samples. Symbols used in both graphs appear in legend, and they are the same as in Fig. 2. Dashed lines in (a) represent the linear fit used to determine the Hall mobility. Continuous lines in (b) represent the classical theoretical prediction.

Then, we considered $\ell_0 = 3\ \mu$m [4] and obtained the triad (R, P, Q) by least square fitting. The continuous line represents the best fit and corresponds to (R, P, Q) = (0.18, 0.0, 0.0). We can see that the theoretical prediction provides a fair representation of the resistivity data. However, when we imposed Q = 1.0, i.e. one completely specular surface, the best fit correspond to (R, P, Q) = (0.24, 0.0, 1.0). It is represented by a dashed line in Fig. 1. In this case, the prediction is not good for thinner samples. If we impose $P = Q = 1.0$ (two completely specular surfaces), then R = 0.29 and the adjusting is worse increasing the difference at lower thickness (theoretical prediction is not shown in Fig. 1).

On the other hand, we determined the resistivity of a sample during the evaporation process. The final thickness of this sample was 120 nm. To compare this behavior with the thickness dependence of the resistivity at 4 K, we measured the resistivity of the 120 nm thick film at 4 K, and we subtracted the difference between the values at RT and at 4 K to all values measured during the deposition process. The thickness dependence of the in situ resistivity is show in Fig. 1 represented by empty circles. For films thicker than 17 nm, we can observe that the behavior of the resistivity measured in situ (empty circles) is very similar to the resistivity of samples measured post-deposition (black squares) and to the theoretical description predicted by MSL (continuous line). However, for 10 nm thick films, the difference reaches one order of magnitude.

Fig. 2a shows the temperature dependence of the resistivity for the five samples labeled with square symbols in Fig. 1.

To study the temperature dependence, we adjusted the grain boundary reflectivity R to obtain the resistivity at 4 K, for each sample. Values of R obtained from this method are indicated in Table 1. They are closer to 0.18 obtained from thickness dependence of the resistivity. Then, we calculated the bulk mean free path $\ell(T) = v_F\tau(T)$, where v_F is the Fermi velocity and $\tau(T)$ is the scattering time calculated from $1/\tau(T) = 1/\tau_{IMP} + 1/\tau_{BG}(T)$, with τ_{IMP} the impurity scattering time, and $\tau_{BG}(T)$ the scattering time obtained from Bloch–Grüneisen theory. Values used were $\tau_{IMP} = 2.16\times 10^{-12}$ s [4] and $\tau_{BG}(T) = m/(nq^2\rho(T))$, where m, n and q are the mass, density, charge of electrons and $\rho(T)$ was obtained from Ref. [14]

In Fig. 2, continuous lines represent theoretical prediction described above for each sample. We can see that they provide a fair representation of temperature dependence of the resistivity between 4 and 70 K.

To compare the resistivity dependence on the temperature for different samples, the temperature coefficient of resistivity (tcr), $\beta(T) = (1/\rho(T))(d_\rho(T)/dT)$, is often used [15]. Fig. 2b shows the ratio of the film tcr to the bulk tcr as a function of the inverse of the α parameter, $\alpha = (\ell_0(T)/D)(R/1-R)$ [11], at 30, 40, 50, 60 and 70 K. Theoretical prediction of data based on MS, was computed from the equation 21 in Ref. [15] (or equation 1.479 in Ref. [16]). Fig. 2b shows these predictions, and we can see good agreement with experimental data, except for the film 33 nm thick, where a slight discrepancy appears. The determination of the temperature dependence of the resistivity at temperatures higher than 70 K seems necessary to elucidate this difference.

Transverse magnetoresistance measurements at 4 K were performed in the five samples labeled with squares in Fig. 1. In 8 and 17 nm thick films, magnetoresistance was null. In 33 and 47 nm thick films, changes appear of about 0.1%, but they are very close to noise level. Only, the film 97 nm thick presents a clear effect about 0·3% at 4.5 T.

Hall voltage V_H was measured in all samples except for 8 nm thick film. From these measurement, we determined Hall tangent and Hall resistance.

Magnetic field dependence of the Hall tangent is displayed in Fig. 3(a). Linear regressions appear as dashed lines. Linear behavior is a fair representation of experimental data, and its slope is the Hall mobility reported in Table 1. Fig. 3(b) shows the magnetic field dependence of the Hall resistance. Continuous lines represent the classical theoretical prediction. We can see that this prediction is good only for the thickest samples, and the discrepancy between theory and experiment increases for thinner films.

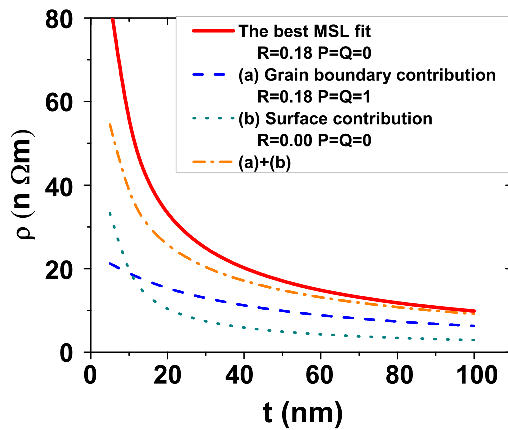

Fig. 4. Comparison of electron surface scattering contribution and electron grain boundary scattering contribution to the resistivity at 4 K, based on MSL theory.

5. Discussion

At 4 K, phonons are frozen out, and then, sample resistivity presents effects of electron surface scattering, electron grain boundary scattering and electron impurities and/or point defects. Quantification of these effects on the resistivity can be performed by the MSL theory through parameters P (or Q), R and ℓ_0. This process can be performed adjusting the thickness dependence of the resistivity.

In the deposition process of our films a high purity gold was used. Then the effect of impurities on the resistivity should be negligible. On the other hand, the effect due to point defects when samples are fabricated at RT and low deposition rate, on the electrical transport can be neglected compared to other scattering mechanisms such as electron-grain boundary and electron-surface [17]. Therefore we used a long mean free path ℓ_0 at 4 K. In order to visualize the contribution of each mechanism, we calculated the resistivity due to electron grain boundary scattering as the MLS prediction for $(R, P, Q) = (0.18, 1.0, 1.0)$, and due to electron surface scattering for $(R, P, Q) = (0.0, 0.0, 0.0)$, i.e. the thickness dependence for films without surfaces, and without grain boundaries, respectively. The comparison appears in Fig. 4.

Fig. 4 shows that electron grain boundary scattering contribution to the resistivity is approximately twice that of electron surface scattering in almost the entire thickness range. For $t \sim 10$ nm, this ratio is broken. This behavior can be explained by the thickness dependence of the mean grain diameter: it presents a minimum of ∼10 nm. As thickness decreases, mean grain diameter diminishes down to ∼10 nm, and since R is constant, the electron grain boundary scattering reduces its effect on the resistivity compared to electron surface scattering, that increases as thickness decreases. This relation between thickness and mean grain diameter was already studied from morphological viewpoint for similar samples elsewhere [2]. On the other hand, performing the addition of resistivity of electron grain boundary scattering and electron surface scattering contributions, the result is always smaller than MSL resistivity prediction, and the difference increases in the thinner limit. The thickness dependence of this addition is represented in Fig. 4 by a dash-dotted line. This increase of the discrepancy as the effect of electron surface scattering grows, has been reported, and the difference was attributed to the interaction between these two scattering mechanism [18].

The behavior of in situ resistance measurements shows a rapid drop of almost two orders of magnitude between 9 and 15 nm, achieving a similar trend as that MSL prediction for $t > 17$ nm. Similar drops have been reported in measurement of sheet resistance during the deposition of gold on SiO_2 at room temperature for 6 nm [19]. The drop is due to transition from an insulating to a metallic state of the films [19].

Temperature dependence of the resistivity, in Fig. 2, shows that its slope decreases as the thickness decreases. This is due to the resistivity at 4 K increasing as thickness decreases, reducing the effect of electron-phonon scattering on the total resistivity. Also, the prediction of the temperature dependence based in the contribution of the bulk phonons is in good agreement with experimental data. In previous works in gold thin films [3,4], an increase in the slope of the temperature dependence over the expected values for bulk phonons have been reported. This increase has been explained as a softening of the phonon modes in the thin film compared to the modes of the bulk. This would appear as a decrease of the Debye temperature, and thereby, an increase in the slope of the temperature dependence. In both reports, this phenomenon appears in gold thin films where the dominant mechanism on the resistivity is electron surface scattering, whereas electron grain boundary scattering is negligible. Therefore, we did not observe this “phonons softening”, because in our films electron grain boundary scattering cannot be ignored.

Regarding transverse magnetoresistance, Table 1 shows values for $(\omega\tau)$ at 4.5 T. We can see that these values are very small. For $(\omega\tau)^2$, we obtained 0.023%, 0.096%, 0.15% and 0.34%, for the film 17, 33, 47 and 97 nm thick, respectively. These values are in good agreement with magnetoresistance of 0.1% and 0.3% measured for the film 47 and 97 nm thick, and show how difficult it is to determine this coefficient in thinner films, where the changes are less than 0.1%. Similar transverse magnetoresistance have been reported in other gold samples: nanoporous thin films [20] and 50 nm thick film composed by nanometric grains [5]. Both reports present values for the resistivity at 4 K which are similar to those found in our samples.

An alternative way to determine the dominant mechanism on the resistivity, independent of the thickness dependence of the resistivity, is to find a linear correlation between Hall mobility and thickness, or Hall mobility and grain diameter [21]. In our samples, we do not have a linear dependence on the thickness or on the grain diameter (graphs not shown), then this method is not applicable. Additionally, in gold thin films it was demonstrated that when the dominant mechanism on the resistivity is the electron surface scattering, the mobilities are $\mu_H \sim \mu_D$[10], but for all our samples $\mu_H > \mu_D$ (see Table 1). To elucidate this problem, we determined the Hall resistivity, and we found that the Hall voltage is larger than the classical prediction in samples where the discrepancy between μ_H and μ_D is higher. Departures from bulk values in the Hall mobility were reported by Chopra et al. [22] in polycrystalline gold films at 77 K. In films with a thickness larger than 60 nm, the Hall mobility achieved the bulk values. In thinner films, they observed thickness dependence of the Hall mobility, where a part was attributed to electron surface scattering modeled through Fuchs–Sondheimer theory [12], and the other, to “enhanced crystallite-size boundary scattering” [22].

6. Conclusions

We determined the thickness dependence of the resistivity, $\rho(t)$, in a set of five gold thin films (8 nm < t < 100 nm) evaporated on mica at room temperature. The theoretical prediction based upon MSL theory for $(R, P, Q) = (0.18, 0.0, 0.0)$ describes fairly well the observed behavior, and indicates that contributions of electron surface scattering and electron grain boundary scattering to the resistivity at 4 K, are comparable in this thickness range. Also, we measured the resistance during the deposition process of a 120 nm thick sample, and determined the in situ resistivity dependence on thickness. The trend is similar to the ex situ determination for $t > 17$ nm.

In the same set of five sample, we determined the temperature dependence of the resistivity, $\rho(T)$, at 4 K < T < 70 K. The temperature dependence can be described by the addition of the contribution of electron scattering from phonons in the bulk.

On the other hand, we measured the Hall Voltage at 4 K in four samples (t = 17, 33, 47, 97 nm) in the presence of a magnetic field, B, up to 4.5 T. We determined the Hall tangent, $tg(\theta)$, the Hall resistance, R_H. Under such conditions, in the four samples, $tg(\theta)$ and R_H present a linear dependence on the magnetic field. From the magnetic field dependence of the Hall tangent, we determined μ_H, which is higher than μ_D in all samples. This behavior can be associated to an increase of the Hall voltage with respect to its bulk value, attributed to the effect of both scattering mechanisms, electron surface scattering and electron grain boundary scattering, acting on this galvanomagnetic coefficient.

Summarizing, the study of the resistivity and the galvanomagnetic coefficients determined at 4 K in gold thin films evaporated at room temperature shows that electron surface scattering and electron grain boundary scattering, contribute in comparable way to electrical transport phenomena, in this thickness range (between 10 nm and 120 nm). Also, we propose a first approximation to the quantification of the effect on the resistivity of each mechanism based on MSL theory. On the other hand, a similar procedure of separation through galvanomagnetic coefficients was not possible.

Acknowledgement

This research was partially supported by CONICYT/CENAVA grant no. 791100037, DGIP-USM grant no. 111353, FONDECYT grant no. 11100277, and PIA Anillo ACT 1117. S. Bahamondes and S. Donoso give thanks for Conicyt Scholarship 22121149 and 22121141. We acknowledge the useful discussion and support of Dr. Raul Munoz.

References

[1] H. Lüth, Solid Surfaces, Interfaces and Thin Films, fifth ed., Springer, 2010.
[2] S. Bahamondes, S. Donoso, R. Henríquez, M. Flores, Thin Solid Films 548 (2013) 646–649.
[3] G. Kästle, H.-G. Boyen, A. Schröder, A. Plettl, P. Ziemann, Phys. Rev. B 70 (2004) 165414.
[4] R. Henriquez, M. Flores, L. Moraga, G. Kremer, C. González-Fuentes, R.C. Munoz, Appl. Surf. Sci. 273 (2013) 315–323.
[5] R. Henriquez, S. Cancino, A. Espinosa, M. Flores, T. Hoffmann, G. Kremer, J.G. Lisoni, L. Moraga, R. Morales, S. Oyarzun, M.A. Suarez, A. Zúñiga, R.C. Munoz, Physical Review B 82 (2010) 113409.
[6] X. Zhang, X. Song, X. Zhang, D. Zhang, Europhys. Lett. 96 (2011) 17010.
[7] D. Goldmayo, J.L. Sacedon, Thin Solid Films 35 (1976) 137–141.
[8] I. Horcas, R. Fernandez, J.M. Gomez-Rodriguez, J. Colchero, J. Gomez-Herrero, A.M. Baro, Rev. Sci. Instrum. 78 (2007) 013705.
[9] G.R. Jones, M. Jackson, K. O'Grady, J. Magn. Magn. Mater. 193 (1999) 75.
[10] R. Henriquez, S. Oyarzun, M. Flores, M. Suarez, L. Moraga, G. Kremer, C.A. Gonzalez-Fuentes, M. Robles, R.C. Munoz, J. Appl. Phys. 108 (2010) 123704.
[11] A.F. Mayadas, M. Shatzkes, Phys. Rev. B 1 (1970) 1382.
[12] E.H. Sondheimer, Adv. Phys. 1 (1952) 1.
[13] M.S.P. Lucas, J. Appl. Phys. 36 (1965) 1632.
[14] R.A. Matula, J. Phys. Chem. Ref. Data 8 (1979) 1147.
[15] C.R. Tellier, A.J. Tosser, Thin Solid Films 44 (1977) 141.
[16] C.R. Tellier, A.J. Tosser, Size Effects in Thin Films, Elsevier Scientific Publishing Company, 1982.
[17] J.M. Heras, E.E. Mola, Thin Solid Films 35 (1976) 75.
[18] E. Broitman, P. Alonso, R. Zimmerman, Thin Solid Films 277 (1996) 192–195.
[19] M. Walther, D.G. Cooke, C. Sherstan, M. Hajar, M.R. Freeman, F.A. Hegmann, Phys. Rev. B 76 (2007) 125408.
[20] T. Fujita, H. Okada, K. Koyama, K. Watanabe, S. Maekawa, Chen and M.W., Phys. Rev. Lett. 101 (2008) 166601.
[21] R. Henriquez, L. Moraga, G. Kremer, M. Flores, A. Espinosa, Raul C. Munoz, Appl. Phys. Lett. 102 (2013) 051608.
[22] K.L. Chopra, S.K. Bahl, J. Appl. Phys. 38 (1967) 3607.